EBioMedicine 36 (2018) 151–158

Contents lists available at ScienceDirect

EBioMedicine

journal homepage: www.ebiomedicine.com

EBioMedicine
Published by THE LANCET

Research paper

Development and validation of a radiomics signature for clinically significant portal hypertension in cirrhosis (CHESS1701): a prospective multicenter study

Fuquan Liu [a,1], Zhenyuan Ning [b,c,1], Yanna Liu [b,1], Dengxiang Liu [d,1], Jie Tian [e], Hongwu Luo [f], Weimin An [g], Yifei Huang [b], Jialiang Zou [b], Chuan Liu [b], Changchun Liu [g], Lei Wang [a], Zaiyi Liu [h], Ruizhao Qi [i], Changzeng Zuo [d], Qingge Zhang [d], Jitao Wang [d], Dawei Zhao [j], Yongli Duan [k], Baogang Peng [l], Xingshun Qi [m], Yuening Zhang [n], Yongping Yang [o], Jinlin Hou [b], Jiahong Dong [p], Zhiwei Li [i,q], Huiguo Ding [n,***], Yu Zhang [c,**], Xiaolong Qi [b,p,r,*]

[a] CHESS Group, Department of Interventional Therapy, Beijing Shijitan Hospital, Capital Medical University, Beijing, China
[b] CHESS Group, Hepatic Hemodynamic Lab, Institute of Hepatology, State Key Laboratory of Organ Failure Research, Nanfang Hospital, Southern Medical University, Guangzhou, China
[c] School of Biomedical Engineering, Southern Medical University, Guangzhou, China
[d] Xingtai People's Hospital, Xingtai Institute of Cancer Control, Xingtai, China
[e] Key Laboratory of Molecular Imaging of Chinese Academy of Sciences, Institute of Automation, Chinese Academy of Sciences, Beijing, China
[f] Department of General Surgery, The Third Xiangya Hospital of Central South University, Changsha, China
[g] Department of Radiology, 302 Hospital of PLA, Beijing, China
[h] Department of Radiology, Guangdong General Hospital, Guangdong Academy of Medical Sciences, Guangzhou, China
[i] Department of General Surgery, 302 Hospital of PLA, Beijing, China
[j] Department of Radiology, Beijing You'an Hospital, Capital Medical University, Beijing, China
[k] Department of Radiology, Beijing Shijitan Hospital, Capital Medical University, Beijing, China
[l] Department of Hepatobiliary Surgery, First Affiliated Hospital of Sun Yat-sen University, Guangzhou, China
[m] Department of Gastroenterology, General Hospital of Shenyang Military Area, Shenyang, China
[n] Department of Gastroenterology and Hepatology, Beijing You'an Hospital, Capital Medical University, Beijing, China
[o] Center for Therapeutic Research of Hepatocarcinoma, 302 Hospital of PLA, Beijing, China
[p] Hepatopancreatobiliary Center, Beijing Tsinghua Changgung Hospital, School of Clinical Medicine, Tsinghua University, Beijing, China
[q] Department of Hepatobiliary Surgery, The Third People's Hospital of Shenzhen, Shenzhen, China
[r] CHESS Frontier Center, Lanzhou University, Lanzhou, China

ARTICLE INFO

Article history:
Received 8 July 2018
Received in revised form 31 August 2018
Accepted 13 September 2018
Available online 27 September 2018

Keywords:
Portal hypertension
Liver cirrhosis
Hepatic venous pressure gradient
Radiomics
Noninvasive

ABSTRACT

Clinically significant portal hypertension (CSPH) is associated with an incremental risk of esophageal varices and overt clinical decompensations. However, hepatic venous pressure gradient (HVPG) measurement, the gold standard for defining CSPH (HVPG≥10 mm Hg) is invasive and therefore not suitable for routine clinical practice. This study aims to develop and validate a radiomics-based model as a noninvasive method for accurate detection of CSPH in cirrhosis.

The prospective multicenter diagnostic trial (CHESS1701, ClinicalTrials.gov identifier: NCT03138915) involved 385 patients with cirrhosis from five liver centers in China between August 2016 and September 2017. Patients who had both HVPG measurement and contrast-enhanced CT within 14 days prior to the catheterization were collected. The noninvasive radiomics model, termed *r*HVPG for CSPH was developed based on CT images in a training cohort consisted of 222 consecutive patients and the diagnostic performance was prospectively assessed in 163 consecutive patients in four external validation cohorts.

*r*HVPG showed a good performance in detection of CSPH with a C-index of 0·849 (95%CI: 0·786–0·911). Application of *r*HVPG in four external prospective validation cohorts still gave excellent performance with the C-index of 0·889 (95%CI: 0·752–1·000, 0·800 (95%CI: 0·614–0·986), 0·917 (95%CI: 0·772–1·000), and 0·827 (95%CI: 0·618–1·000), respectively. Intraclass correlation coefficients for inter- and intra-observer agreement were 0·92–0·99 and 0·97–0·99, respectively.

* Correspondence to: X. Qi, CHESS Group, Hepatic Hemodynamic Lab, Institute of Hepatology, Nanfang Hospital, Southern Medical University, 1838 North Guangzhou Avenue, Guangzhou 510515, China.
** Correspondence to: Y. Zhang, School of Biomedical Engineering, Southern Medical University, Guangzhou, China.
*** Correspondence to: H. Ding, Department of Gastroenterology and Hepatology, Beijing You'an Hospital, Capital Medical University, Beijing, China.
E-mail addresses: dinghuiguo@ccmu.edu.cn (H. Ding), yuzhang@smu.edu.cn (Y. Zhang), qixiaolong@vip.163.com (X. Qi).
[1] These authors contributed equally to this work.

https://doi.org/10.1016/j.ebiom.2018.09.023

A radiomics signature was developed and prospectively validated as an accurate method for noninvasive detection of CSPH in cirrhosis. The tool of *r*HVPG assessment can facilitate the identification of CSPH rapidly when invasive transjugular procedure is not available.

1. Introduction

Clinically significant portal hypertension (CSPH) in cirrhosis, defined as a hepatic venous pressure gradient (HVPG) ≥ 10 mmHg, is associated with an incremental risk of esophageal varices, overt clinical decompensation and development of hepatocellular carcinoma [1–3]. However, the HVPG measurement is invasive and available only in specialized hepatology units [4–6]. Herein a noninvasive tool capable of identifying CSPH would definitely be of great benefit for better stratifying patients with cirrhosis and decompensation outcomes [7–9].

To date, in patients with compensated advanced chronic liver disease, liver stiffness measured by transient elastography is the most commonly used noninvasive method to predict CSPH. However, concerns regarding the unreliable measurement of liver stiffness in patients with obesity and necrotic inflammation, and the influence of collaterals information towards liver stiffness are brought out [5,10,11]. In addition, liver stiffness measurement is not recommended in the diagnosis of cirrhosis in adults with nonalcoholic fatty liver disease [12]. The diagnostic performance of other noninvasive models for CSPH in cirrhosis is still controversial, such as CT-based portal pressure ($HVPG_{CT}$) score [13], portal diameter, aspartate aminotransferase (AST) to alanine aminotransferase (ALT) ratio (AAR) [14], AST to and platelet count (PLT) ratio index (APRI) [15], and fibrosis index based on four factors (FIB-4) [16].

Radiomics technique converts images into a high dimensional mineable feature space using various automatically extracted data-characterization algorithms [17–19]. Numerous studies have applied the emerging radiomics technique to improve diagnostic, prognostic, and predictive accuracy of cancer research [20–23]. To our best knowledge, there is no literature describing a radiomics signature that could facilitate the noninvasive detection of CSPH in cirrhosis. Therefore, the study aims to develop and validate an easy-to-use radiomics signature, which we termed radiomics-based hepatic venous pressure gradient (*r*HVPG), as a noninvasive method for accurate detection of CSPH in cirrhosis.

Research in context

Evidence before this study

- Clinically significant portal hypertension (CSPH) is associated with an incremental risk of clinical decompensations.
  - Hepatic venous pressure gradient (HVPG) measurement, the gold standard for defining CSPH is invasive and therefore not suitable for routine clinical practice. A noninvasive tool capable of detecting CSPH is urgently needed.
  - Radiomics-based technique has shown potential in noninvasive diagnosis of liver fibrosis.

Added value of this study

We developed and prospectively validated a radiomics signature, termed *r*HVPG as an accurate method for noninvasive detection of CSPH in cirrhosis.

Implications of all the available evidence

The tool of radiomics-based hepatic venous pressure gradient (*r*HVPG) assessment can facilitate the identification of CSPH rapidly when invasive transjugular procedure is not available.

2. Materials and methods

2.1. Patients

This is a prospective multicenter diagnostic trial (CHESS1701, ClinicalTrials.gov identifier: NCT03138915), which involved 385 consecutive eligible patients with cirrhosis of various etiologies from five liver centers in China between August 2016 and September 2017. The training cohort was recruited from the 302 Hospital of PLA while the external validation cohorts involved patients from Beijing Shijitan Hospital, Beijing Youan Hospital, Xingtai People's Hospital, and Third Xiangya Hospital. Inclusion criteria were: 1) patients who were diagnosed of liver cirrhosis; 2) patients who had HVPG measurement and abdominal contrast-enhanced CT scan; 3) adult patients (age ≥ 18 years); 4) written informed consent. Exclusion criteria included: 1) patients who previously underwent one of the following surgical procedures: transjugular intrahepatic porto-systemic shunt, splenectomy, partial splenic embolization, balloon-occluded retrograde, transvenous obliteration, or liver transplantation; 2) patients with confirmed hepatocellular carcinoma based on histologic examination of liver or combined chronic liver disease history, radiologic and laboratory findings; 3) patients with non-sinusoidal portal hypertension (e.g. hepatic cavernoma, Budd-chiari syndrome); 4) pregnant patients. All the enrolled patients underwent standardized clinical examinations including contrast-enhanced CT scan, serum tests and so on. CT was conducted within 14 days prior to the transjugular HVPG measurement while the laboratory assessments were conducted at the day before the catheterization. The study was performed according to Helsinki declaration and approved by all institutional review board.

2.2. Transjugular HVPG measurement

The transjugular HVPG measurement was performed by experienced interventional radiologists according to the standard protocol [24]. The Balloon catheter (Edwards Lifesciences, Irvine, California) with a pressure transducer at the tip was used. A zero measurement with the transducer open to air was needed before the study. The free hepatic venous pressure was measured as the balloon catheter was placed at the ostium of the right hepatic vein close to the inferior vena cava (approximately 1–3 cm). Then as the balloon was inflated for total occlusion of the right hepatic vein, the wedged hepatic venous pressure was measured. Continuous recording was necessary until the pressure reached a plateau. All measurements were performed in triplicate and then averaged. The HVPG was the difference between the wedged hepatic venous pressure and the free hepatic venous pressure.

2.3. CT image acquisition

All patients underwent contrast-enhanced CT scan using one of the following systems: Discovery CT750 HD (GE Healthcare), LightSpeed VCT (GE Healthcare), Brilliance iCT (Philips Healthcare), or Sensation 16 CT (Siemens). The following parameters were used: tube voltage, 120 kVp or 100kVp; tube current, 150–600 mA; slice thickness, 1.25 mm; pitch, 1.375. All patients received an intravenous, nonionic contrast medium (iodine concentration, 370 mg/mL; volume, 1.5–2.0 ml/kg of body weight; contrast type, Iopromide Injection, Bayer Pharma AG) at a rate of 3–5 ml/s. A volume of 20 ml saline was injected after the injection of the contrast.

2.4. Radiomics feature extraction and rHVPG development

Portal venous-phase CT images (DICOM format) were transferred to technicians for radiomics feature extraction in a blinded fashion. Region of interest (ROI) were delineated around the liver at the porta hepatis level and around the spleen at the splenic hilum level using ITK-SNAP 3·6 (ITK-SNAP 3·X TEAM) (Fig. 1a). Then, ROIs were imported into the Matlab 2016b (Mathworks, Natick, USA) with feature extraction algorithms implemented. In order to achieve high throughput features, both texture and non-texture features extractions were conducted (Fig. 1b). Particularly, preprocessing of the ROI images, that is, image normalization including Wavelet band-pass filtration, isotropic resampling and quantization of gray level were needed before the texture feature extraction process. To overcome the overfitting, the least absolute shrinkage and selection operator (LASSO) regression model, a popular method for regression with high-dimensional predictors, was used to select the most predictive features and build the signature (Fig. 1c) [20]. The value of the radiomics signature was computed for each patient through a linear combination of selected features weighted by their respective coefficients (see Supplementary Materials for details).

2.5. Inter-observer and intra-observer reliability assessment

The inter-observer reliability was analyzed with 100 randomly and equiprobably chosen cases in a blinded fashion by two independent technicians (reader 1: Huang Y.; reader 2: Zou J.) for ROI segmentation and radiomics feature extraction. Besides, to study the intra-observer agreement, one technician (Huang Y.) repeated the above procedures twice on the same cases with a two-week interval between the two readings to reduce the recall bias. A χ^2 test was used to assess the differences between the ROI and features attained by reader 1 and those by reader 2. Intraclass correlation coefficient (ICC) was computed to evaluate the inter- and intra-observer agreement.

2.6. Imaging-based and serum-based models

Three imaging-based indexes including liver stiffness by FibroScan (Echosens, France), portal diameter and $HVPG_{CT}$ score were assessed. $HVPG_{CT}$ score was calculated as: $HVPG_{CT} = 17{\cdot}37–4{\cdot}91*\ln(\text{Liver/-Spleen volume ratio}) + 3{\cdot}8$ [if presence of peri-hepatic ascites] [13]. Portal diameter was measured by Doppler Ultrasound (Philips iU22 Ultrasound System, New York). In addition, three serum biomedical indexes, including AST, ALT, and PLT were measured with a conventional automated analyzer at the day of HVPG measurement. AAR, APRI and FIB-4 were calculated by the formulas as follow: AAR = AST/ALT [14]. APRI = AST(/upper limit of normal)/PLT($\times 10^9$/L) × 100 [15]. FIB-4 = [age × AST(U/L)]/[PLT($\times 10^9$/L) × ALT(U/L)$^{1/2}$] [16].

2.7. Statistical analysis

Categorical data was expressed as numbers (percentages) and continuous variables as mean (standard deviation). A Chi-square test was used to assess the effect of the clustering analysis. The reducing dimensions method, the LASSO [20] and binary logistic regression were performed using the "glmnet" package (R language 3·0·2, R Core Team, 2013). The diagnostic performance of *r*HVPG was assessed using C-index after 1000 bootstrap resamples. C-index was calculated using the "Hmisc" package. Receiver operating characteristic curves was performed using the "pROC" package. The cutoff values for diagnosing CSPH in cirrhosis were defined as maximal sum of sensitivity and specificity. Chi-square test, *t*-test and ICC were calculated using Matlab 2016b (Mathworks, Natick, USA) with "ICC" function supplemented. Back derivation of the *r*HVPG function and barplot were performed using Matlab with built-in functions. A *P*-value < 0·05 was considered statistically significant.

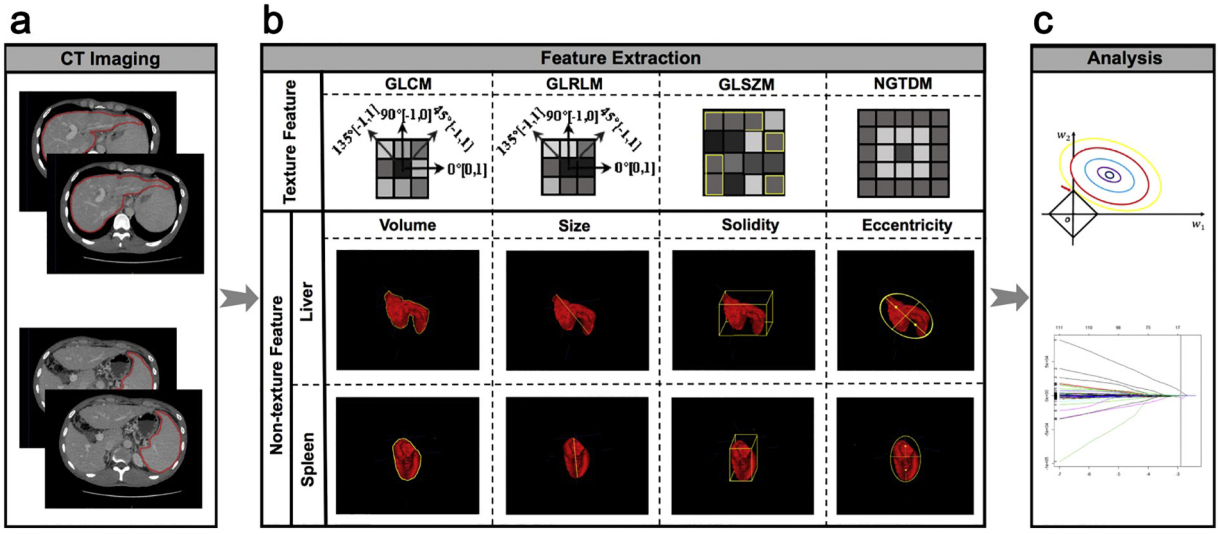

Fig. 1. Workflow for the radiomics process. (a) Segmentation of region of interest on CT images. (b) Extraction of both texture and non-texture features. (c) Radiomics feature selection using the least absolute shrinkage and selection operator regression model. CT, computed tomography; GLCM, Gray-level co-occurence matrix; GLRLM, Gray-level run-length matrix; GLSZM, Gray-level size zone matrix; NGTDM, Neighborhood gray-level difference matrix.

3. Results

3.1. Study population

A total of 385 patients with liver cirrhosis from 5 liver centers were enrolled in this prospective multicenter trial. Two hundred and forty-three consecutive eligible patients were collected from the 302 Hospital of PLA, among which nine patients were excluded because of non-evaluable or incomplete CT images, and 12 patients were excluded during radiomics feature extraction due to the reading failure for CT slice thickness, resulting in 222 patients included in the training cohort to build the *r*HVPG signature (Fig. 2). Additionally, 163 eligible patients were prospectively recruited from four external centers (the Beijing Shijitan Hospital, Beijing Youan Hospital, Xingtai People's Hospital, and Third Xiangya Hospital) as validation cohorts (Fig. 2). Baseline characteristics of study population were outlined in Table 1.

3.2. Radiomics feature selection and rHVPG development

After extracting features from ROIs, 20,648 radiomics features were retrieved from portal venous-phase CT images and then reduced to 11 potential predictors with seven features from liver and four from spleen using the LASSO regression analysis (Fig. 3a and 3b). The *r*HVPG signature was established using LASSO model based on the 11 radiomics features including SumAverge (n = 2), Gray-Level Variance (n = 2), Run-Length Variance (n = 1), Zone Percentage (n = 2), Small Zone Low Gray-Level Emphasis (n = 2), Large Zone Low Gray-Level Emphasis (n = 1), and Zone-Size Variance (n = 1). Distribution of the *r*HVPG

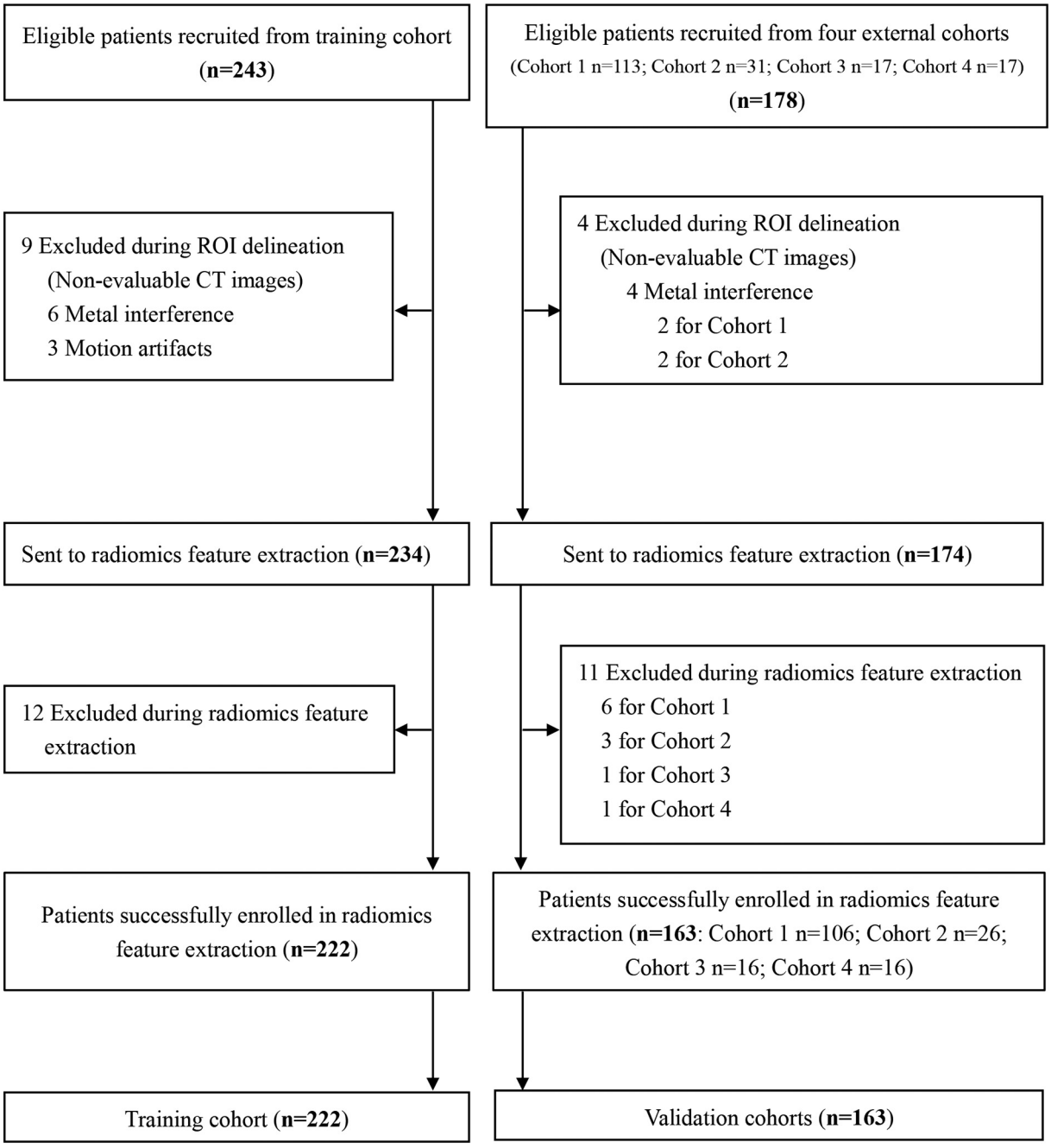

Fig. 2. Flow diagram for study enrollment. ROI, region of interest. Training cohort: The 302 Hospital of PLA. Validation cohorts: Cohort 1: Beijing Shijitan Hospital; Cohort 2: The Third Xiangya Hospital; Cohort 3: Beijing Youan Hospital; Cohort 4: Xingtai People's Hospital.

Table 1
Baseline characteristics in the training and validation cohorts.

Variables	Training cohort (n = 222)	Validation cohorts (n = 163)			
		Cohort 1 (n = 105)	Cohort 2 (n = 26)	Cohort 3 (n = 16)	Cohort 4 (n = 16)
Age, mean (SD), year	48 (11)	54 (12)	48 (12)	47 (11)	48 (11)
Male, n (%)	151 (68·0%)	76 (72·4%)	19 (73.1%)	8 (50·0%)	10 (62·5%)
BMI, mean (SD), kg/m^2	23·0 (3·1)	23.0 (3·3)	22·9 (3·0)	22 (3·9)	24·8 (4·3)
HVPG, mean (SD), mmHg	16·1 (6·1)	24.7 (10·9)	15·1 (5·1)	11·4 (5.8)	13·0 (4·1)
HVPG ≥10 mmHg, n (%)	182 (82·0%)	101 (96·2%)	21 (80·8%)	11 (68·8%)	12 (75·0%)
Etiology, n (%)					
Hepatitis B virus	169 (76·1%)	71 (67·6%)	21 (80·8%)	9 (56·3%)	8 (50·0%)
Alcohol	17 (7·7%)	11 (10·5%)	1 (3·8%)	2 (12·5%)	2 (12·5%)
Hepatitis C virus	9 (4·1%)	5 (4·8%)	0	0	3 (18·8%)
Other	27 (12·2%)	18 (17·1%)	4 (15·3%)	5 (31·3%)	3 (18·8%)
Child-Pugh score, n (%)					
Class A	181 (81·5%)	4 (3·8%)	18 (69·2%)	10 (62·5%)	9 (56·3%)
Class B	34 (15·3%)	75 (71·4%)	7 (26·9%)	4 (25·0%)	3 (18·8%)
Class C	7 (3·2%)	26 (24·8%)	1 (3·8%)	2 (12·5%)	4 (25·0%)
AST (μkat/L), mean (SD)	0·64 (0·39)	0.58 (0.37)	0·91 (1·13)	0·58 (0·31)	0·49 (0·18)
ALT (μkat/L), mean (SD)	0·48 (0·35)	0·42 (0·31)	0·98 (1·71)	0·61 (0·27)	0·45 (0·37)
Albumin (g/L), mean (SD)	35·5 (4·3)	35·4 (5·7)	35·4 (4·9)	39·4 (6·3)	37·3 (5·5)
TBIL (μmol/L), mean (SD)	19·2 (11·9)	27·6 (18·5)	24·7 (27·0)	23·6 (10·5)	28·2 (12·4)
INR, mean (SD)	1·15 (0·14)	1·3 (0·2)	1·4 (0·39)	1·37 (0·22)	1·21 (0·16)
PLT (10^9/L), mean (SD)	93·4 (104·7)	83·3 (53·0)	182·2 (215·7)	54·0 (34·1)	83·5 (54·5)

SD, standard deviation; y, year; BMI, body mass index; HVPG, hepatic venous pressure gradient; AST, aspartate aminotransferase.
ALT, alanine aminotransferase; TBIL, total bilirubin; INR, international normalized ratio; PLT, platelet count.

values and the CSPH status determined by invasive HVPG values was shown in Fig. S1. Notably, there was no statistical difference between *r*HVPG-based and HVPG-based classification (P > 0·05). ICC values for inter- and intra-observer agreement assessment ranged from 0·92–0·99 and 0·97–0·99, respectively, suggesting the robust reliability and reproducibility of *r*HVPG.

3.3. Diagnostic performance of rHVPG for CSPH

In the training cohort (n = 222), the *r*HVPG signature showed a good diagnostic performance for detection of CSPH (HVPG≥10 mmHg as reference standard) in cirrhosis with the C-index, sensitivity, specificity, positive predictive value and negative predictive value of 0·849 (95%CI: 0·786–0·911), 78·7% (95%CI: 73·2%-84·7%), 76·9% (95%CI: 64·1%-89·7%), 94·1% (95%CI: 91·1%-97·3%), and 43·5% (95%CI: 36·3%-51·7%), respectively (Table 1). Applying a cut-off of *r*HVPG = 0·81 for diagnosis of CSPH, 77·9% (173/222) of the cases were correctly identified as CSPH or non-CSPH with HVPG as reference (Table S1).

Compared to the imaging-based and serum-based noninvasive models including liver stiffness by FibroScan (n = 53), $HVPG_{CT}$ score (n = 177), portal diameter (n = 220), AAR (n = 222), APRI (n = 222) and FIB-4 (n = 222), the *r*HVPG signature still showed the highest diagnostic performance. The area under the receiver operating characteristic curves (AUCs) for *r*HVPG and aforementioned noninvasive models were 0·849 (95%CI: 0·786–0·911), 0·778 (95%CI: 0·618–0·938), 0·549 (95%CI: 0·442–0·656), 0·505 (95%CI: 0·396–0·613), 0·473 (95%CI: 0·378–0·568), 0·558 (95%CI: 0·456–0·660), 0·483 (95%CI: 0·382–0·584), respectively (Fig. 4).

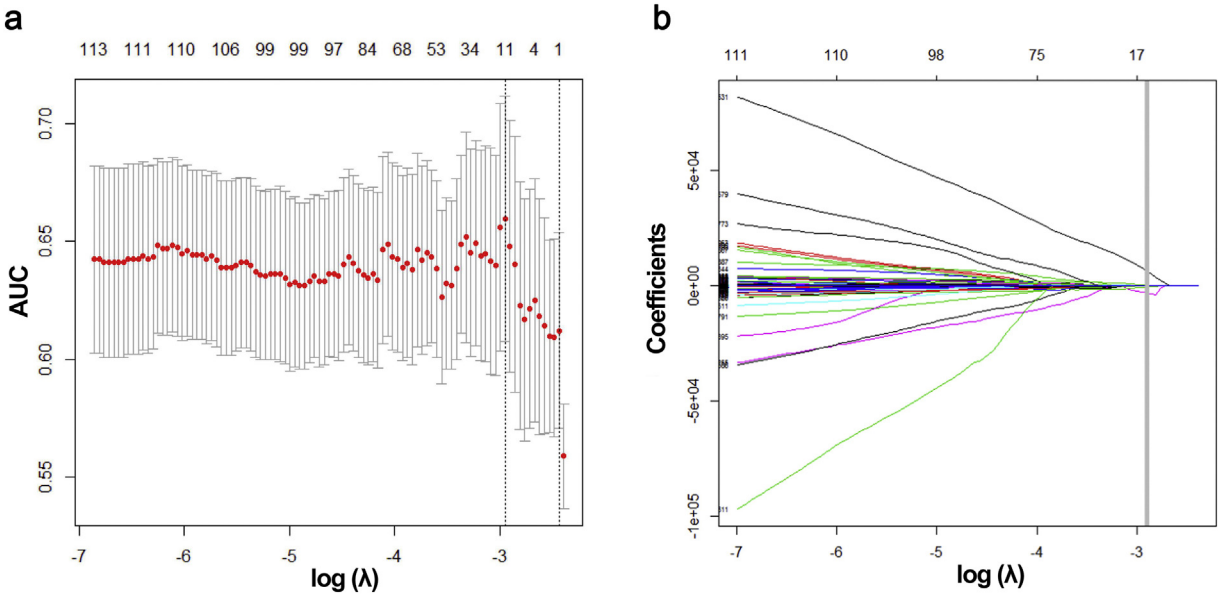

Fig. 3. Radiomics feature selection using the least absolute shrinkage and selection operator (LASSO) regression model. (a) Tuning parameter (λ) selection in LASSO model used ten-fold cross-validation via minimum criteria. Dotted vertical lines were drawn both at the optimal (left) and minimum values (right) by using minimum criteria and 1 standard error of minimum criteria. A λ value of 0.0525, with log (λ), −2·947 was chosen using ten-fold cross-validation. (b) LASSO coefficient profiles of 20,648 features. A coefficient profile plot was produced versus the log (λ) sequence. Vertical line was drawn at the value selected where optimal λ resulted in 11 nonzero coefficients.

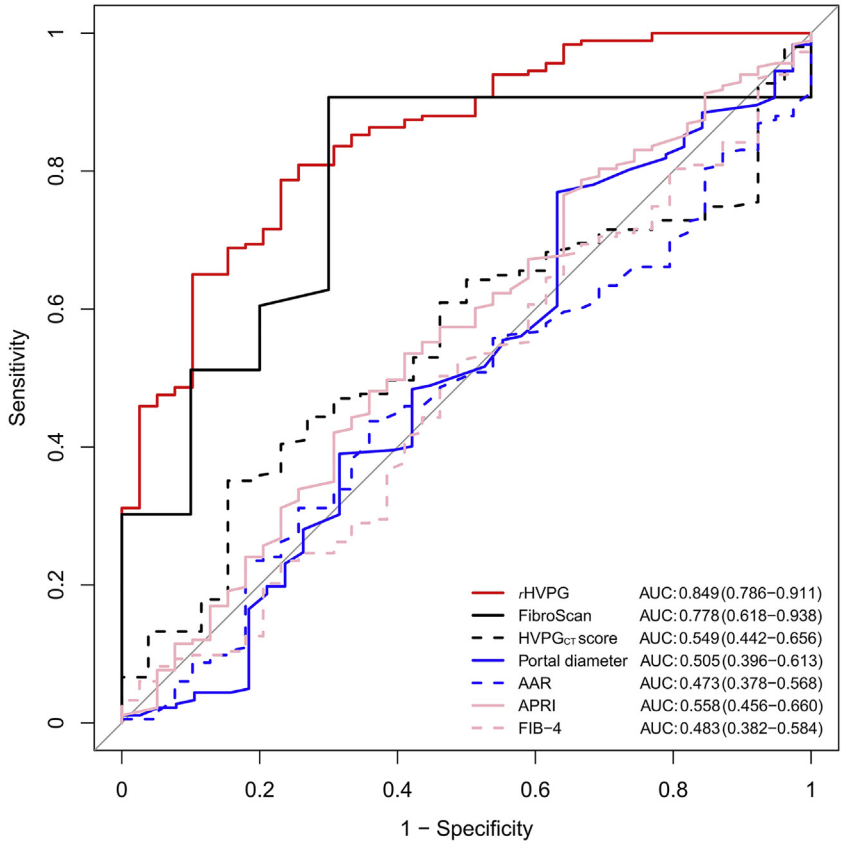

Fig. 4. Receiver operating characteristic curves of the *r*HVPG and other noninvasive models for detection of clinically significant portal hypertension in cirrhosis. *r*HVPG, radiomics-based hepatic venous pressure gradient.

Cutoff values, sensitivity, specificity, positive predictive value, and negative predictive value of all noninvasive tests for the diagnosis of CSPH in cirrhosis were summarized in Table 2.

3.4. Validation of the diagnostic performance of rHVPG for CSPH

In the prospective validation, *r*HVPG signature exhibited a satisfied performance for CSPH (HVPG ≥ 10 mmHg as reference) in four external independent cohorts with the C-index of 0·889 (95%CI: 0·752–1·000), 0·800 (95%CI: 0·614–0·986), 0·917 (95%CI: 0·772–1·000), and 0·827 (95%CI: 0·618–1·000), respectively (Fig. 5). Besides, the sensitivity and specificity for each validation cohort were 69·3% (95%CI: 58·4%-76·2%) and 100% (95%CI: 100%–100%), 85·7% (95%CI: 71·4%–100%) and 80·0% (95%CI: 40·0%–100%), 83·3% (95%CI: 58·3%–100%) and 100% (95%CI: 100%–100%), 63·6% (95%CI: 36·4%-90·9%) and 100% (95%CI: 100%–100%), respectively. The positive predictive value and negative predictive value of validation cohorts for the diagnosis of CSPH in cirrhosis were summarized in Table 3.

4. Discussion

Noninvasive tools for CSPH detection in cirrhosis have been highlighted in recent years, especially in regions where the invasive HVPG measurement is not readily accessible. In the study, we proposed a radiomics signature and demonstrated that the noninvasive signature had an excellent diagnostic performance for CSPH in patients with cirrhosis.

In this prospective study, we applied radiomics technique in the diagnosis of portal hypertension and validated the radiomics signature in four external independent cohorts while previous work failed to do so [20–23]. Machine learning is an advanced technology now being widely used in the diagnosis of various diseases for status classification [25,26]. The noninvasive radiomics signature based on a machine learning method with the competence to recognize the deeper pattern, which we termed *r*HVPG, was developed from 222 consecutive cirrhotic patients and externally validated in 163 eligible cases. The C-index of *r*HVPG signature for CSPH was generally satisfied throughout the training and four external validation cohorts, suggesting that *r*HVPG could

Table 2
Performance of *r*HVPG and other noninvasive models in diagnosing clinically significant portal hypertension in cirrhosis in the training cohort.

	*r*HVPG	FibroScan, kPa	$HVPG_{CT}$ score	Portal diameter, mm	AAR	APRI	FIB-4
AUC (95%CI)	84·9 (78·6–91·1)	77·8 (61·8–93·8)	54·9 (44·2–65·6)	50·5 (39·6–61·3)	47·3 (37·8–56·8)	55·8 (45·6–66·0)	48·3 (38·2–58·4)
Cutoff	0.81	14·2	19·1	14·6	1·46	1·34	5·00
Sensitivity (95%CI)	78·7 (73·2–84·7)	90·7 (81·4–97·7)	35·1 (27·2–43·1)	76·9 (70·9–83·0)	43·7 (36·6–51·4)	53·6 (46·5–60·7)	50·3 (43·2–57·4)
Specificity (95%CI)	76·9 (64·1–89·7)	70·0 (40·0–100·0)	84·6 (69·2–96·2)	36·8 (21·1–52·6)	64·1 (48·7–79·5)	59·0 (43·6–74·4)	53·8 (38·5–69·2)
PPV (95%CI)	94·1 (91·1–97·3)	92·9 (86·7–100·0)	93·0 (86·5–98·3)	85·4 (82·1–88·5)	85·1 (79·4–90·7)	86·0 (80·7–90·8)	83·6 (78·5–88·6)
NPV(95%CI)	43·5 (36·3–51·7)	63·6 (42·9–90·0)	18·3 (15·3–21·4)	25·0 (15·4–34·6)	19·5 (15·3–23·7)	21·3(15·8–26·6)	18·8 (13·8–23·8)

*r*HVPG, radiomics-based hepatic venous pressure gradient; $HVPG_{CT}$ score, CT-based portal pressure score; CT, computed tomography; AAR, aspartate aminotransferase to alanine aminotransferase ratio; FIB-4, fibrosis index based on 4 factors; APRI, aspartate aminotransferase to platelet count ratio index; AUC, the area under the receiver operating characteristic curve; PPV, positive predictive value; NPV, negative predictive value.

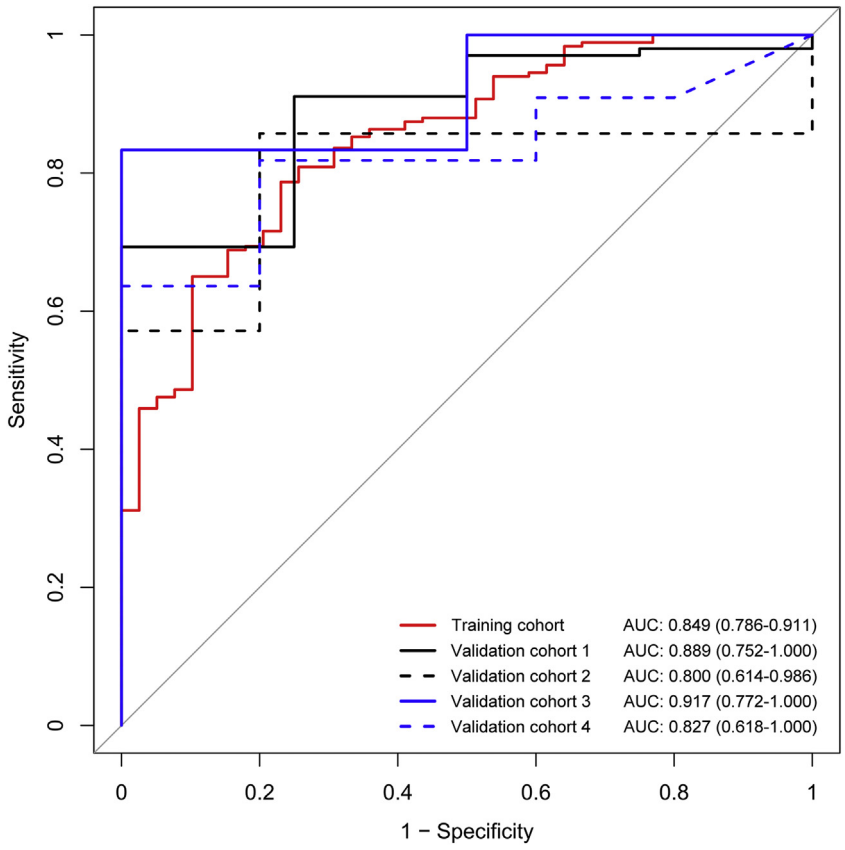

Fig. 5. Receiver operating characteristic curves of the *r*HVPG for detection of clinically significant portal hypertension in cirrhosis in the training and validation cohorts. *r*HVPG, radiomics-based hepatic venous pressure gradient.

accurately facilitate the detection of CSPH in cirrhosis, which implies the development of more-advanced stages.

Liver stiffness by FibroScan has been the most validated noninvasive surrogate measurement of HVPG to identify CSPH in cirrhosis [5,6,27]. In the study, FibroScan performed better than other imaging-based and serum-based models for CSPH detection, which was consistent with previous studies [27,28]. However, the diagnostic accuracy of FibroScan for CSPH was not quite satisfactory with the AUC of 0·778 (95%CI: 0·618–0·938). Our HBV-dominant (72·2%, 278/385) cirrhotic cohort might explain this slight fluctuation. Acute exacerbation occurs more frequently in HBV patients, in which the overestimated liver stiffness by FibroScan tends to parallel with the degree of necroinflammation, corroborated by the reports showing significant correlation between the falsely high liver stiffness with increased alanine aminotransferase levels and the decrease of liver stiffness during the recovery phase [29,30]. It is also noted that patients with obesity are associated with unreliable liver stiffness measurement by FibroScan [5,6,27], which is not the limitation of *r*HVPG signature. Also, the accuracy of liver stiffness by FibroScan might be hindered by severe portal hypertension because the increasingly relevance of extrahepatic factors such as collateral formation in disease progression [30,31]. Moreover, a recent study has emphasized the disconnection of portal pressure in further progression stage of cirrhosis [10]. Therefore, we suggested that *r*HVPG signature might be served as an auxiliary parameter for FibroScan. However, further studies are needed to explore the effect of necroinflammation and obesity on the accuracy of *r*HVPG.for identifying CSPH in cirrhosis.

Important benefits of the *r*HVPG signature are safety and reproducibility with the fact that HVPG measurement was greatly limited by the invasive procedure and therefore not suitable for dynamic monitoring [4–6]. Besides, the correlation analysis showed that there was no statistically significant correlation between *r*HVPG and the clinical indexes including age, AST, ALT, PLT, ALB, TBIL, and INR. Clinical physicians only need to upload CT images and select the ROI to perform the radiomics analysis and help to determine whether a patient with cirrhosis has the CSPH or not, and then facilitate clinical decision-making.

A potential criticism of our study is that the prevalence of CSPH is high, which may bring the doubt of the optimal cut-off value of *r*HVPG signature. However, in the present study, a better performance of *r*HVPG for identifying CSPH was observed in validation cohort 3 with a less ratio of CSPH (68·8%). The proposed radiomics signature needs to be further validated in more participants with mild portal hypertension. Rigorously designed studies are planned in well characterized cohorts of patients with compensated cirrhosis and well-defined etiologies.

Table 3
Performance of *r*HVPG in diagnosing clinically significant portal hypertension in cirrhosis in the training and validation cohorts.

	Training cohort (n = 222)	Validation cohort 1 (n = 105)	Validation cohort 2 (n = 26)	Validation cohort 3 (n = 16)	Validation cohort 4 (n = 16)
AUC (95%CI)	0·849 (0·786–0·911)	0·889 (0·752–1·000)	0·800 (0·614–0·986)	0·917 (0·772–1·000)	0·827 (0·618–1·000)
Sensitivity (95%CI)	0·787 (0·732–0·847)	0·693 (0·584–0·762)	0·857 (0·714–1·000)	0·833 (0·583–1·000)	0·636 (0·364–0·909)
Specificity (95%CI)	0·769 (0·641–0·897)	1·000 (1·000–1·000)	0·800 (0·400–1·000)	1·000 (1·000–1·000)	1·000 (1·000–1·000)
PPV (95%CI)	0·941 (0·911–0·973)	1·000 (1·000–1·000)	0·947 (0·857–1·000)	1·000 (1·000–1·000)	1·000 (1·000–1·000)
NPV (95%CI)	0·435 (0·363–0·517)	0·114 (0·087–0·143)	0·571 (0·333–1·000)	0·667 (0·444–1·000)	0·556 (0·417–0·833)

*r*HVPG, radiomics-based hepatic venous pressure gradient; AUC, the area under the receiver operating characteristic curve; PPV, positive predictive value; NPV, negative predictive value.

Another limitation of our study was that emerging noninvasive techniques such as magnetic resonance elastography [32] and liver surface nodularity quantification [33] were not studied. A future study comparing radiomics with other radiologic methods is needed.

In conclusion, a radiomics signature, termed *r*HVPG, was developed and prospectively validated as an accurate method for noninvasive detection of CSPH in cirrhosis. The tool of *r*HVPG assessment can facilitate the identification of CSPH rapidly when invasive procedure is not available.

Acknowledgement

This work was supported by the grants from National Natural Science Foundation of China (81600510, 81672725); Guangdong Science Fund for Distinguished Young Scholars (2018B030306019); Guangzhou Industry-Academia-Research Collaborative Innovation Major Project (201704020015); Special Funds for the Cultivation of Guangdong College Students' Scientific and Technological Innovation (pdjha0096); Beijing Municipal Administration of Hospitals Clinical Medicine Development of Special Funding (ZYLX201610), Beijing Municipal Administration of Hospitals' Ascent Plan (DFL20151602), Application Research on Clinical Characteristics of the Capital (z161100000516197), Capital's Funds for Health Improvement and Research (2018-1-2081). The funders had no involvement in the study design, data collection and analysis, decision to publish, or preparation of the manuscript. The corresponding authors (Xiaolong Qi & Yu Zhang & Huiguo Ding) have full access to all the data in the study and had final responsibility for the decision to submit for publication.

Declaration of interests

No author has any potential conflict to disclose (financial, professional or personal) relevant to the manuscript.

Author contributions

Study concept and design: Qi X, Zhang Y, Ding H. Acquisition of data: An W, Wang L, Qi R, Liu CC, Zhang YN, Zhao D, Duan Y, Liu C, Zuo C, Zhang Q, Wang J. Technique support: Zhang Y, Tian J, Liu Z, Yang Y, Hou J, Dong J. Analysis and interpretation of data: Ning Z, Huang Y, Zou J, Peng B, Qi XS. Drafting of the manuscript: Qi X, Liu Y. Critical revision of the manuscript: Liu F, Ding H, Liu D, Li Z, Luo H.

Appendix A. Supplementary data

Supplementary data to this article can be found online at https://doi.org/10.1016/j.ebiom.2018.09.023.

References

[1] Tsochatzis EA, Bosch J, Burroughs AK. Liver cirrhosis. Lancet 2014;383(9930):1749–61.
[2] Garcia-Tsao G, Bosch J. Management of varices and variceal hemorrhage in cirrhosis. N Engl J Med 2010;362(9):823–32.
[3] García-Pagán JC, Caca K, Bureau C, et al. Early use of TIPS in patients with cirrhosis and variceal bleeding. N Engl J Med 2010;362(25):2370–9.
[4] Bosch J, Abraldes JG, Berzigotti A, et al. The clinical use of HVPG measurements in chronic liver disease. Nat Rev Gastroenterol Hepatol 2009;6(10):573–82.
[5] Garcia-Tsao G, Abraldes JG, Berzigotti A, et al. Portal hypertensive bleeding in cirrhosis: risk stratification, diagnosis, and management: 2016 practice guidance by the American Association for the study of liver diseases. Hepatology 2017;65:310–35.
[6] de Franchis R, Faculty Baveno VI. Expanding consensus in portal hypertension: report of the Baveno VI Consensus Workshop: Stratifying risk and individualizing care for portal hypertension. J Hepatol 2015;63:743–52.
[7] Abraldes JG, Bureau C, Stefanescu H, et al. Noninvasive tools and risk of clinically significant portal hypertension and varices in compensated cirrhosis: the "Anticipate" study. Hepatology 2016;64:2173–84.
[8] Qi X, Li Z, Huang J, et al. Virtual portal pressure gradient from anatomic CT angiography. Gut 2015;64:1004–5.
[9] Qi X, Berzigotti A, Cardenas A, Sarin SK. Emerging non-invasive approaches for diagnosis and monitoring of portal hypertension. Lancet Gastroenterol Hepatol 2018;3(10):708–19.
[10] Piecha F, Paech D, Sollors J, et al. Rapid change of liver stiffness after variceal ligation and TIPS implantation. Am J Physiol Gastrointest Liver Physiol 2018;314(2):G179–87.
[11] Tana MM, Muir AJ. Diagnosing liver fibrosis and cirrhosis: serum, imaging or tissue? Clin Gastroenterol Hepatol 2018;16(1):16–8.
[12] Lim JK, Flamm SL, Singh S, et al. Clinical guidelines committee of the American gastroenterological association. American gastroenterological association institute guideline on the role of elastography in the evaluation of liver fibrosis. Gastroenterology 2017;152:1536–43.
[13] Iranmanesh P, Vazquez O, Terraz S, et al. Accurate computed tomography-based portal pressure assessment in patients with hepatocellular carcinoma. J Hepatol 2014;60:969–74.
[14] Castéra L, Le Bail B, Roudot-Thoraval F, et al. Early detection in routine clinical practice of cirrhosis and oesophageal varices in chronic hepatitis C: comparison of transient elastography (FibroScan) with standard laboratory tests and non-invasive scores. J Hepatol 2009;50(1):59–68.
[15] Wai CT, Greenson JK, Fontana RJ, et al. A simple noninvasive index can predict both significant fibrosis and cirrhosis in patients with chronic hepatitis C. Hepatology 2003;38:518–26.
[16] Vallet-Pichard A, Mallet V, Nalpas B, et al. FIB-4: an inexpensive and accurate marker of fibrosis in HCV infection comparison with liver biopsy and fibrotest. Hepatology 2007;46(1):32–6.
[17] Lambin P, Leijenaar RTH, Deist TM, et al. Radiomics: the bridge between medical imaging and personalized medicine. Nat Rev Clin Oncol 2017;14(12):749–62.
[18] Gillies RJ, Kinahan PE, Hricak H. Radiomics: Images are more than pictures, they are data. Radiology 2016;278:563–77.
[19] Dong J, Qi X. Liver imaging in precision medicine. EBioMedicine 2018;32:1–2.
[20] Huang YQ, Liang CH, He L, et al. Development and validation of a radiomics romogram for preoperative prediction of lymph node metastasis in colorectal cancer. J Clin Oncol 2016;34:2157–64.
[21] Huang Y, Liu Z, He L, et al. Radiomics signature: A potential biomarker for the prediction of disease-free survival in early-stage (I or II) non-small cell lung cancer. Radiology 2016;281:947–57.
[22] Liu Z, Zhang X, Shi Y, et al. Radiomics analysis for evaluation of pathological complete response to neoadjuvant chemoradiotherapy in locally advanced rectal cancer. Clin Cancer Res 2017;23(23):7253–62.
[23] Zhang B, Tian J, Dong D, et al. Radiomics features of multiparametric MRI as novel prognostic factors in advanced nasopharyngeal carcinoma. Clin Cancer Res 2017;23(15):4259–69.
[24] Groszmann RJ, Wongcharatrawee S. The hepatic venous pressure gradient: anything worth doing should be done right. Hepatology 2004;39(2):280–2.
[25] Ehteshami Bejnordi B, Veta M, Johannes Van Diest P, et al. Diagnostic assessment of deep learning algorithms for detection of lymph node metastases in women with breast cancer. JAMA 2017;318:2199–210.
[26] Esteva A, Kuprel B, Novoa RA, et al. Dermatologist-level classification of skin cancer with deep neural networks. Nature 2017;542:115–8.
[27] Berzigotti A. Non-invasive evaluation of portal hypertension using ultrasound elastography. J Hepatol 2017;67:399–411.
[28] Lemoine M, Shimakawa Y, Nayagam S, et al. The gamma-glutamyl transpeptidase to platelet ratio (GPR) predicts significant liver fibrosis and cirrhosis in patients with chronic HBV infection in West Africa. Gut 2016;65:1369–76.
[29] Fraquelli M, Rigamonti C, Casazza G, et al. Etiology-related determinants of liver stiffness values in chronic viral hepatitis B or C. J Hepatol 2011;54:621–8.
[30] Qi X, Liu F, Li Z, et al. Insufficient accuracy of computed tomography-based portal pressure assessment in hepatitis B virus-related cirrhosis: An analysis of data from CHESS-1601 trial. J Hepatol 2017;68(1):210–1.
[31] Shung DL, Garcia-Tsao G. Liver capsule: portal hypertension and varices: pathogenesis, stages and management. Hepatology 2017;65(3):1038.
[32] Gharib AM, Han MAT, Meissner EG, et al. Magnetic resonance elastography shear wave velocity correlates with liver fibrosis and hepatic venous pressure gradient in adults with advanced liver disease. Biomed Res Int 2017;2017:2067479.
[33] Smith AD, Branch CR, Zand K, et al. Liver surface nodularity quantification from routine CT images as a biomarker for detection and evaluation of cirrhosis. Radiology 2016;280(3):771–81.